Deep Defects Seen on Visual Fields Spatially Correspond Well to Loss of Retinal Nerve Fiber Layer Seen on Circumpapillary OCT Scans

Maria A. Mavrommatis,[1] Zhichao Wu,[1] Saskia I. Naegele,[1] Jason Nunez,[1] Carlos Gustavo de Moraes,[2] Robert Ritch,[3] and Donald C. Hood[1]

[1]Department of Psychology, Columbia University Visual Science Lab, New York, New York, United States
[2]Department of Ophthalmology, Columbia University, New York, New York, United States
[3]Department of Ophthalmology, New York Eye and Ear Infirmary, New York, New York, United States

Correspondence: Donald C. Hood, Department of Psychology, 406 Schermerhorn Hall, 1190 Amsterdam Avenue MC 5501, New York, NY 10027, USA; dch3@cumc.columbia.edu.

Submitted: October 4, 2017
Accepted: December 21, 2017

Citation: Mavrommatis MA, Wu Z, Naegele SI, et al. Deep defects seen on visual fields spatially correspond well to loss of retinal nerve fiber layer seen on circumpapillary OCT scans. *Invest Ophthalmol Vis Sci*. 2018;59:621–628. https://doi.org/10.1167/iovs.17-23097

Purpose. To examine the structure–function relationship in glaucoma between deep defects on visual fields (VF) and deep losses in the circumpapillary retinal nerve fiber layer (cpRNFL) on optical coherence tomography (OCT) circle scans.

Methods. Thirty two glaucomatous eyes with deep VF defects, as defined by at least one test location worse than ≤ -15 dB on the 10-2 and/or 24-2 VF pattern deviation (PD) plots, were included from 87 eyes with "early" glaucoma (i.e., 24-2 mean deviation better than −6 dB). Using the location of the deep VF points and a schematic model, the location of local damage on an OCT circle scan was predicted. The thinnest location of cpRNFL (i.e., deepest loss) was also determined.

Results. In 19 of 32 eyes, a region of complete or near complete cpRNFL loss was observed. All 19 of these had deep VF defects on the 24-2 and/or 10-2. All of the 32 eyes with deep VF defects had abnormal cpRNFL regions (red, 1%) and all but 2 had a region of cpRNFL thickness <21 μm. The midpoint of the VF defect and the location of deepest cpRNFL had a 95% limit of agreement within approximately two-thirds of a clock-hour (or 30°) sector (between −22.1° to 25.2°). Individual fovea-to-disc angle (FtoDa) adjustment improved agreement in one eye with an extreme FtoDa.

Conclusions. Although studies relating local structural (OCT) and functional (VF) measures typically show poor to moderate correlations, there is good qualitative agreement between the location of deep cpRNFL loss and deep defects on VFs.

Keywords: glaucoma, visual field, optical coherence tomography, structure-function

Glaucoma is a progressive optic neuropathy that results in loss of retinal ganglion cells (RGCs).[1] There is no single litmus test for glaucoma, and clinicians and researchers alike have yet to achieve a consensus regarding the best tools to evaluate the disease, although it is generally agreed that both functional and structural tests should be included. Currently, a visual field (VF) test, using standard automated perimetry (SAP), is the most common method to quantify functional loss in glaucoma,[2,3] and optical coherence tomography (OCT) is increasingly being used as a structural test, most commonly through measuring the circumpapillary retinal nerve fiber layer (cpRNFL).[3–6]

Several studies have demonstrated that a statistically significant structure–function relationship exists between these two clinical tests.[7–13] In general, these studies report moderate correlations at best. This relatively poor level of correlation is affected by measurement error of the structural and functional tests, individual differences in retinal anatomy and visual function, and the topographic relationship (map) between them.[8,11,13–19] To improve the correlation between VFs and OCT, Ganeshrao et al.[15] reduced measurement error by averaging two VF tests and four OCT tests and used individualized maps relating OCT to VF. However, the best correlation was only 0.56. Interestingly, considering the 30° cpRNFL region most affected in each individual improved the correlation to 0.72. Of course, this still leaves 48% of the variance unexplained.

A number of previous studies have focused on this unexplained variance, which has been attributed to factors, such as failure of the computer algorithm to properly segment the cpRNFL; variation in individual mapping of retinal locations to disc regions; the presence of a nonneural, residual cpRNFL; the spacing of the visual field points, and so on.[8,11,13–19] Here, we focus instead on the extent to which structural and functional abnormalities agree when eyes with deep defects seen on VFs (i.e., pattern deviation [PD] ≤ -15dB) and/or on OCT circle scans (i.e., loss of local cpRNFL) are compared. From a practical perspective, this study should help the clinician interpret the VF and OCT results involving deep defects.

Methods

Participants

This prospective study evaluated 32 eyes with glaucoma from 31 participants that had "deep" VF defects, in which "deep"

was defined as having at least one location on the PD plot less than or equal to −15 dB when VF testing was performed using either the Swedish Interactive Threshold Algorithm (SITA) standard 24-2 or 10-2 testing strategy on a Humphrey Field Analyzer II-I (Carl Zeiss Meditec, Inc., Dublin, CA, USA). The eyes were among a larger group of 204 eyes that had abnormal or suspicious appearing discs, mean deviation (MD) values better than −6 dB on 24-2 VF testing, and spherical refractive errors within ± 6D. Of these 204 eyes, 87 were judged to have glaucomatous damage by two glaucoma specialists based upon optic disc stereo-photographs, 24-2 and 10-2 VFs, an inner retinal report based upon a single wide-field OCT scan (described in detail in a previous study[20]), and other clinical information (including family history of glaucoma, history of intraocular surgery, and IOP and corneal thickness measurements). Of these 87 eyes, 34 had deep VF defects as described above, and two were excluded due to lack of recent VF testing.

This study was approved by the institutional review boards of Columbia University and New York Eye and Ear Infirmary of Mount Sinai and followed the tenets of the Declaration of Helsinki and the Health Insurance Portability and Accountability Act. Written informed consent was obtained from all the participants in this study following an explanation of all test procedures.

Optical Coherence Tomography Imaging

A high-resolution circle scan was obtained for all eyes in this study using a spectral-domain (SD) OCT device (3D OCT-2000, Topcon, Inc., Tokyo, Japan) and was manually centered on the optic disc during acquisition. The circle scan was 3.4 mm in diameter, and consisted of 1024 A-scans and 50 frames were averaged for each scan. VFs and OCT circle scans were within 6 months of each other.

Predicting the Circumpapillary RNFL Location of Damage From the Deep VF Points

To evaluate the spatial correspondence between deep visual field defects and regions of cpRNFL thinning on OCT circle scans, the 10-2 and 24-2 VF test point locations were morphed to account for the displacement of RGCs near fixation[20–23] and then overlaid on a schematic model,[24,25] as shown in Figures 1A and 1B. According to the model in Figure 1A, the region of RGCs associated with the temporal half of the disc (solid black circle) falls within the red and blue contours; the dashed black circle is the location of the OCT circle scan. Deep 24-2 VF test points, defined by ≤ −15 dB on the PD plot, were enclosed within a contour (red contour in Fig. 1A). Figure 1B shows the region of the retina, and the region of the disc and circle scan, associated with RGCs in the macula (blue circle: ±8° from fixation) and macular papillary region. Deep 10-2 VF test points (≤ −15 dB on the PD plot) were enclosed within a contour (green contour in Fig. 1B).

The red and green contours achieved from the 24-2 and 10-2 VFs, respectively (Figs. 1A, 1B), were then superimposed on the anatomic model combined with the RNFL bundle tracings of Jansonius et al.[26] in Figure 1C. The location of damage on the circle scan was predicted, as shown in Figure 1C by the red slanted lines. A compass was superimposed on the center of the disc (represented by the smaller dashed circle) in Figure 1C and the location of the slanted lines on the dashed circle measured using the temporal most point as a reference (i.e., 9 o'clock for the right eye was 0°). The location of these red lines was then translated via degree-to-millimeter conversion to the SD-OCT circle scans as shown in Figure 2A (red vertical lines), and the midpoint of these lines is indicated by the red circle. The region marked by the red vertical lines represents the model's prediction of the location of structural damage on the OCT circle scan associated with the deep VF locations.

Two of the authors (MM and JN) performed this procedure independently, and the 95% limits of agreement for widths and midpoints of the VF prediction were −18.7° to 15.9° and −16.6° to 15.6° respectively, or approximately within half a clock-hour (or 30°) sector. The location of thinnest cpRNFL (i.e., deepest loss) was also determined (yellow circles in Fig. 2A), and the 95% limits of agreement between two observers were −17.3° to 18.7°.

The Circumpapillary RNFL Location of Deep Damage

Without taking into consideration the VF prediction of damage, the location of thinnest cpRNFL region on the OCT circle scan was determined qualitatively as indicated by the double-ended yellow arrow in Figures 2A and 2B, and the midpoint of the region was then determined (yellow circle). For eyes in which the thinnest cpRNFL encompassed a very small region, the yellow circle indicates the entire width of the defect, as in Figures 2C through 2E.

In addition to the identification of the thinnest cpRNFL region, all eyes were categorized as having either complete or nearly complete cpRNFL loss, or incomplete cpRNFL loss. A region was defined as having complete or nearly complete cpRNFL loss if the thinnest location was less than 10 μm as in Figures 2A through 2C and incomplete loss if thinning relative to the 5% normal limits was present, but the average thickness was greater than 10 μm as in Figures 2D and 2E. The same two authors also performed this evaluation independently and agreed on all classifications.

Results

Level of Spatial Agreement Between Structure and Function

All 32 eyes with deep VF defects had a focal region of abnormality on the OCT circle scan, with at least one region of cpRNFL thickness that fell below the 1% normal limits. Of the 32 eyes, 19 had a region of complete or nearly complete cpRNFL loss, examples of which can be seen in Figures 2A through 2C. Interestingly, these 19 eyes were the only eyes with complete or nearly complete loss of the cpRNFL in the total sample of 87 abnormal eyes. In other words, a deep VF defect was always observed in eyes with either complete or nearly complete local cpRNFL loss in this dataset.

The remaining 15 eyes were categorized as having incomplete cpRNFL loss. In 13 of 15 eyes with incomplete damage, only a relatively thin (<21 μm) region was present (e.g., Figs. 2D, 2E). The remaining two eyes were the only ones with a reasonably thick region, although still abnormal at the 1% level, as seen in Figure 3. Notice that in both of these eyes, fewer than two points were ≤ −15 dB on the 24-2 (left panel in Figs. 3A, 3D) and none were on the 10-2 (right panel in Figs. 3A, 3D), and they tended to be in the periphery of the 24-2 VF (red outlines on Fig. 3A, 3D).

The midpoint of the VF defect (red circle in Figs. 2, 3) and the location of deepest cpRNFL loss (yellow circle in Figs. 2, 3) exhibited spatial agreement within two-thirds of a 30° clock hour (range, 0.0°–30.3°; 95% limits of agreement −22.1° to 25.2°) as shown by the Bland-Altman plot in Figure 4A. However, in 2 of 32 cases, the region of thinnest RNFL (yellow circle) fell outside the VF prediction (red vertical lines). These two eyes share a very interesting quality: the disc-to-fovea angle was extreme (either very large or very small).

Investigative Ophthalmology & Visual Science

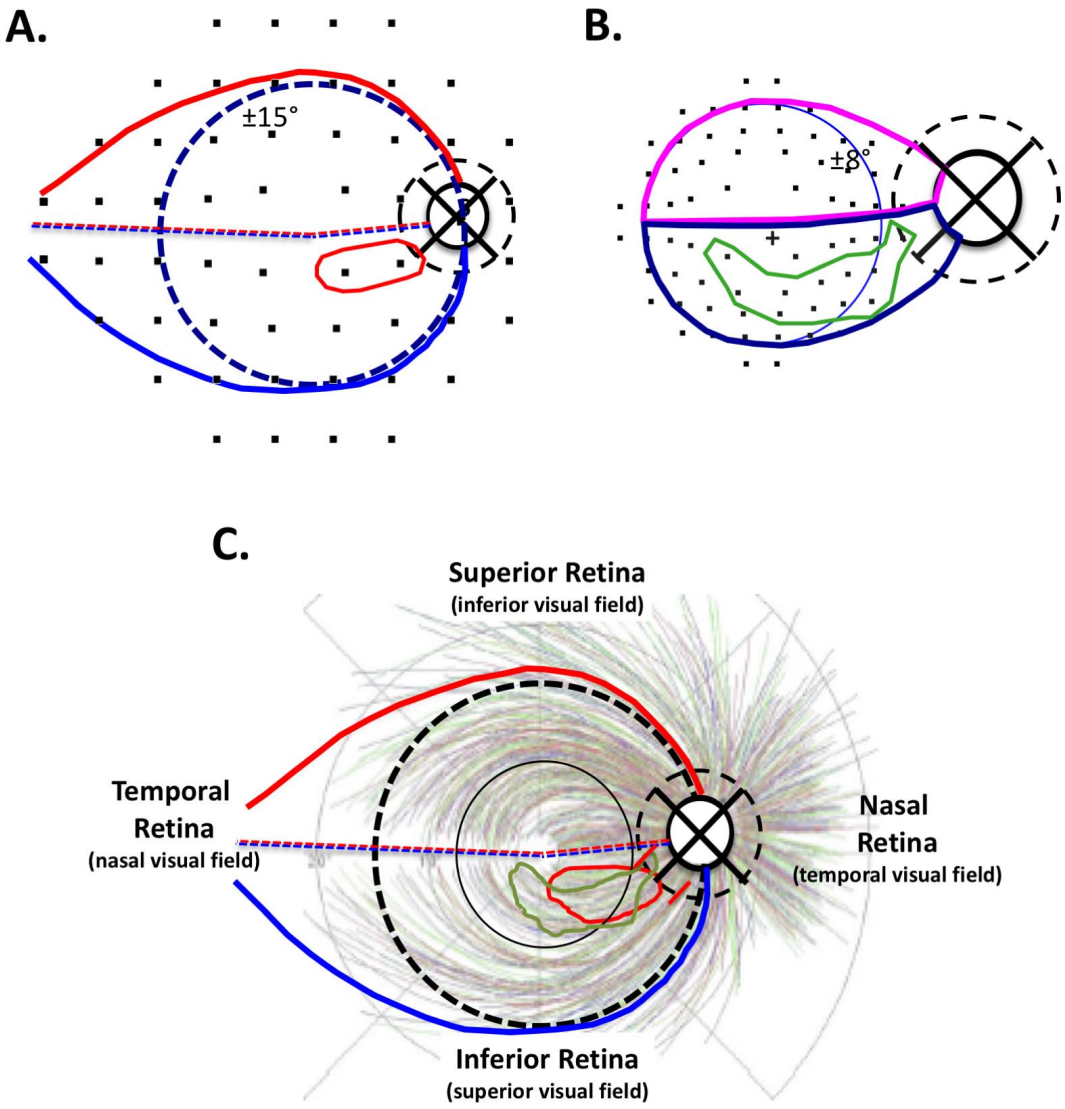

FIGURE 1. (**A**, **B**) 24-2 (**A**) and 10-2 (**B**) VF points were overlaid on the anatomic model, creating a map linking functional damage on the VF to cpRNFL structural damage.[19] VF pattern deviation values ≤ −15 dB were enclosed within a contour to indicate the region of deepest functional loss (*red* and *green contours* in [**A**] and [**B**], respectively). (**C**) Based on the location of 10-2 and 24-2 deep damage (*red* and *green contours*) and the Jansonius et al.[26] bundle tracings, *red slanted lines* were drawn on the *dashed circle* representing the location of the circumpapillary scan of the optic disc. This represented a VF-based prediction of structural damage.

Impact of Adjustments of the Disc-to-Fovea Angle

Previous studies have suggested that the structure–function relationship could improve by using individualized mapping.[14,15] Therefore, we evaluated the impact of adjusting the VF-predicted region of damage (red lines and circles in Figs. 2, 3) for each eye based on the difference between its disc-to-fovea angle and the average angle of this cohort (8.0°). The 95% limits of agreement were similar with and without such adjustments (−22.0° to 25.2° and −22.1° to 25.2°, respectively), indicating that at a cohort level, the disc-to-fovea adjustment yielded little difference in structure–function agreement; the limits of agreement are illustrated using Bland-Altman plots (Fig. 4A).

While individualized adjustment for disc-to-fovea angle yielded little change in the level of structure–function agreement at the population level, we observed that it did show improvements in certain cases. Figure 4B shows the swept-source (SS) OCT average voxel projection slab (AVP-slab) en face of one of the two eyes in which the midpoint of the thinnest cpRNFL fell outside the VF prediction. This eye had a disc-to-fovea angle of 0.89°, well below the group's average of 8.0°. The disc-to-fovea adjustment (red dashed vertical lines and white circle in Fig. 4C) improved structure–function agreement so that the region of structural damage fell within the corrected VF prediction.

DISCUSSION

This study sought to determine the level of spatial agreement between deep structural and functional defects in glaucomatous eyes when using OCT imaging and VF testing. By using an anatomic model to trace deep VF test locations ≤ −15 dB back to the optic disc, we were able to predict the location of deepest cpRNFL loss within two-thirds of a 30° clock hour sector, or roughly 20°, in 91.4% of cases. Thus, although studies relating local structural (OCT) and functional (VF) measures

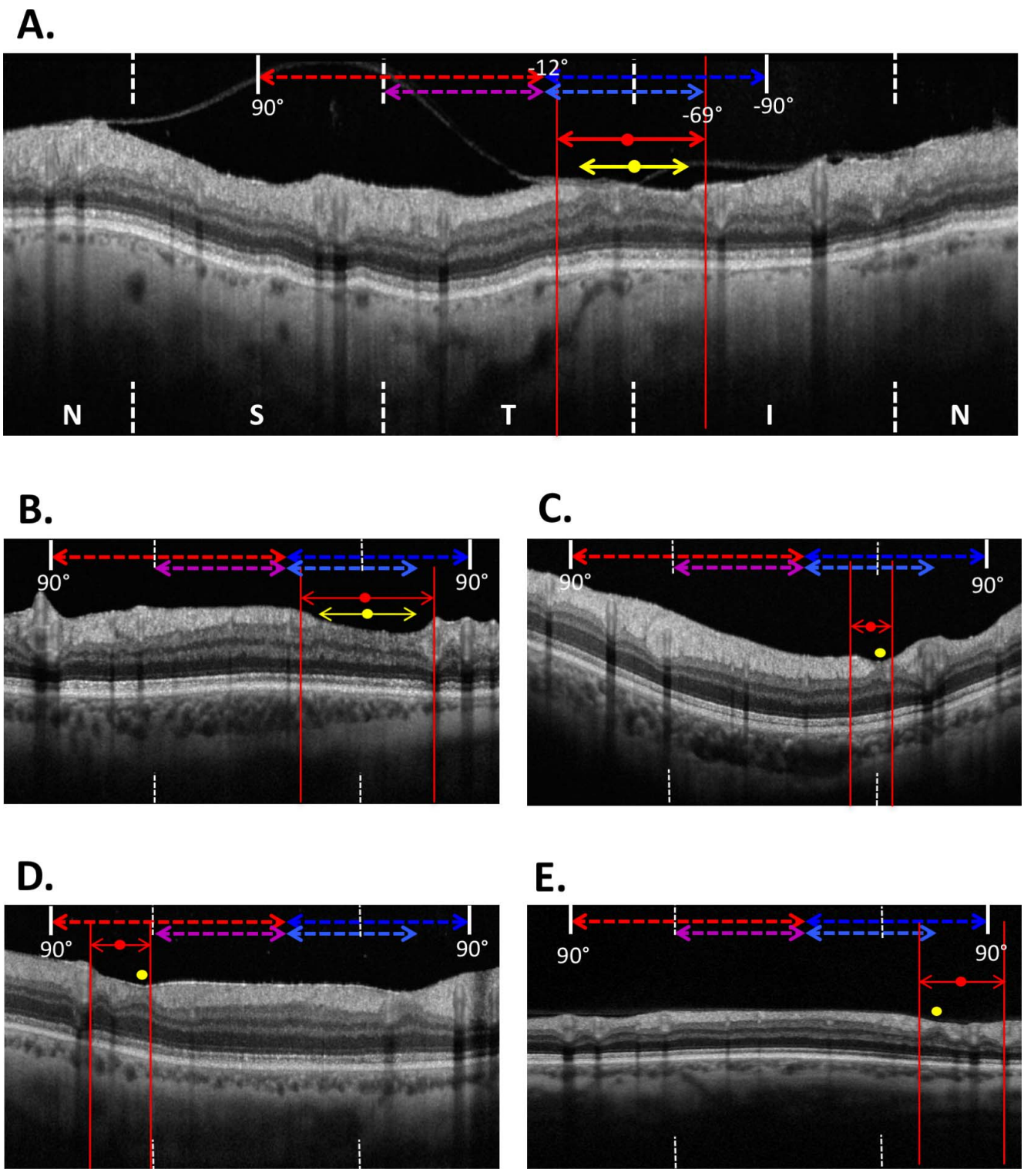

FIGURE 2. (**A**) The *red slanted lines* in Figure 1C were translated to the nasal, superior, temporal, inferior, nasal (NSTIN) cpRNFL OCT scans and presented as *red solid vertical lines with arrows*. The *red circle* indicated the midpoint of this line, while the point of thinnest cpRNFL was indicated by a *yellow circle*. (**B**, **C**) Along with (**A**), examples of eyes that exhibited complete local cpRNFL dropout. (**D**, **E**) Examples of eyes that exhibited incomplete local cpRNFL loss (<21 μm in thickness). Note the scan images in (**B**–**E**) include the central ±90°.

typically show poor to moderate correlations, there is good qualitative agreement between the location of deep cpRNFL loss and deep defects on VFs. Further, these findings provide important insights into the level of spatial agreement that can be expected for these two clinical tests when interpreting their results during the clinical management of patients with glaucoma.

In this study, we observed that all eyes with deep VF defects also had a local region of cpRNFL abnormality on OCT imaging, defined as a region where the cpRNFL thickness fell below the

Investigative Ophthalmology & Visual Science

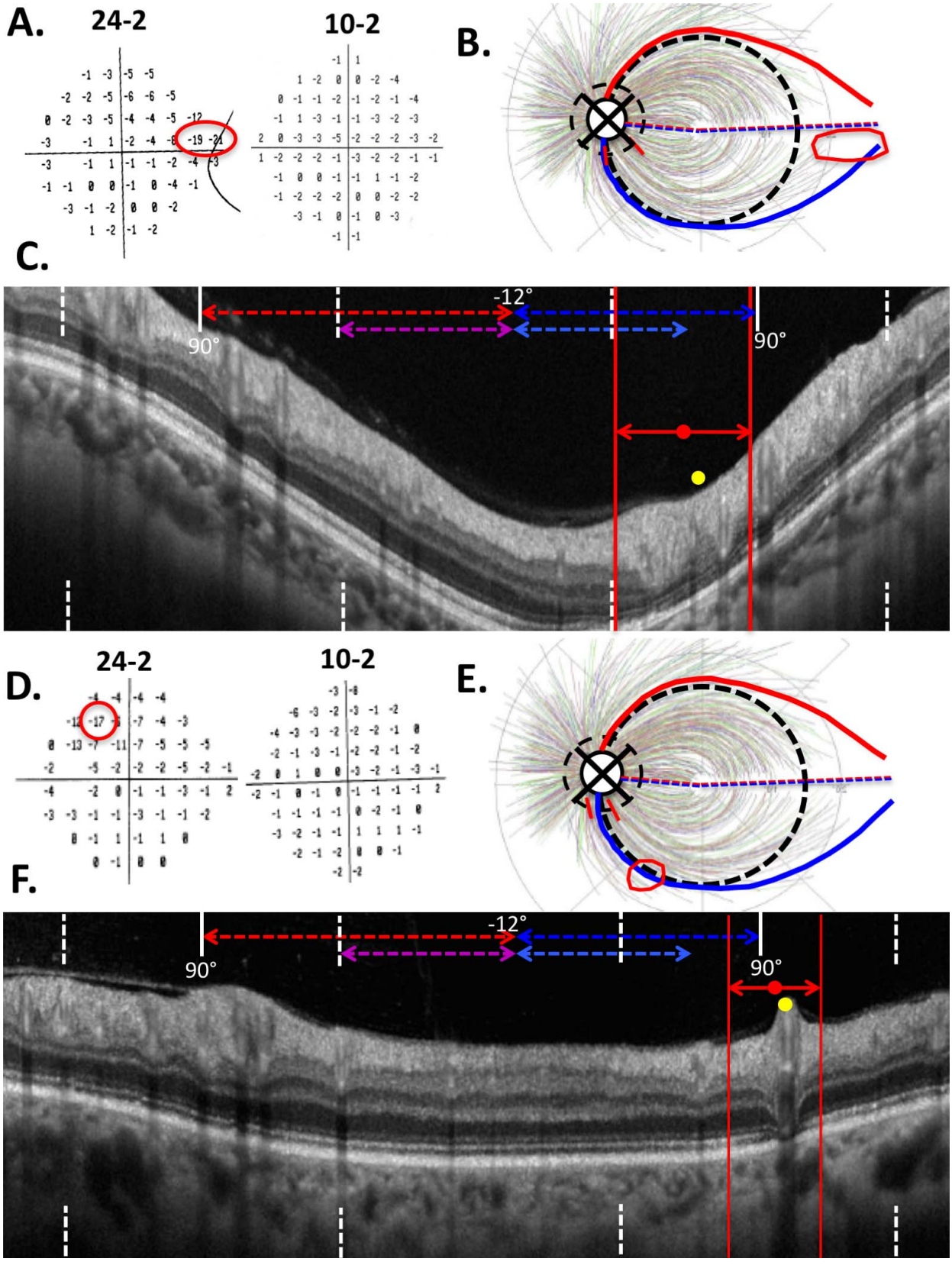

Figure 3. The two eyes that had considerable cpRNFL thickness in the anticipated area of damage based on the VF. The 24-2 of both eyes had only one or two deep test points, while the 10-2 had none.

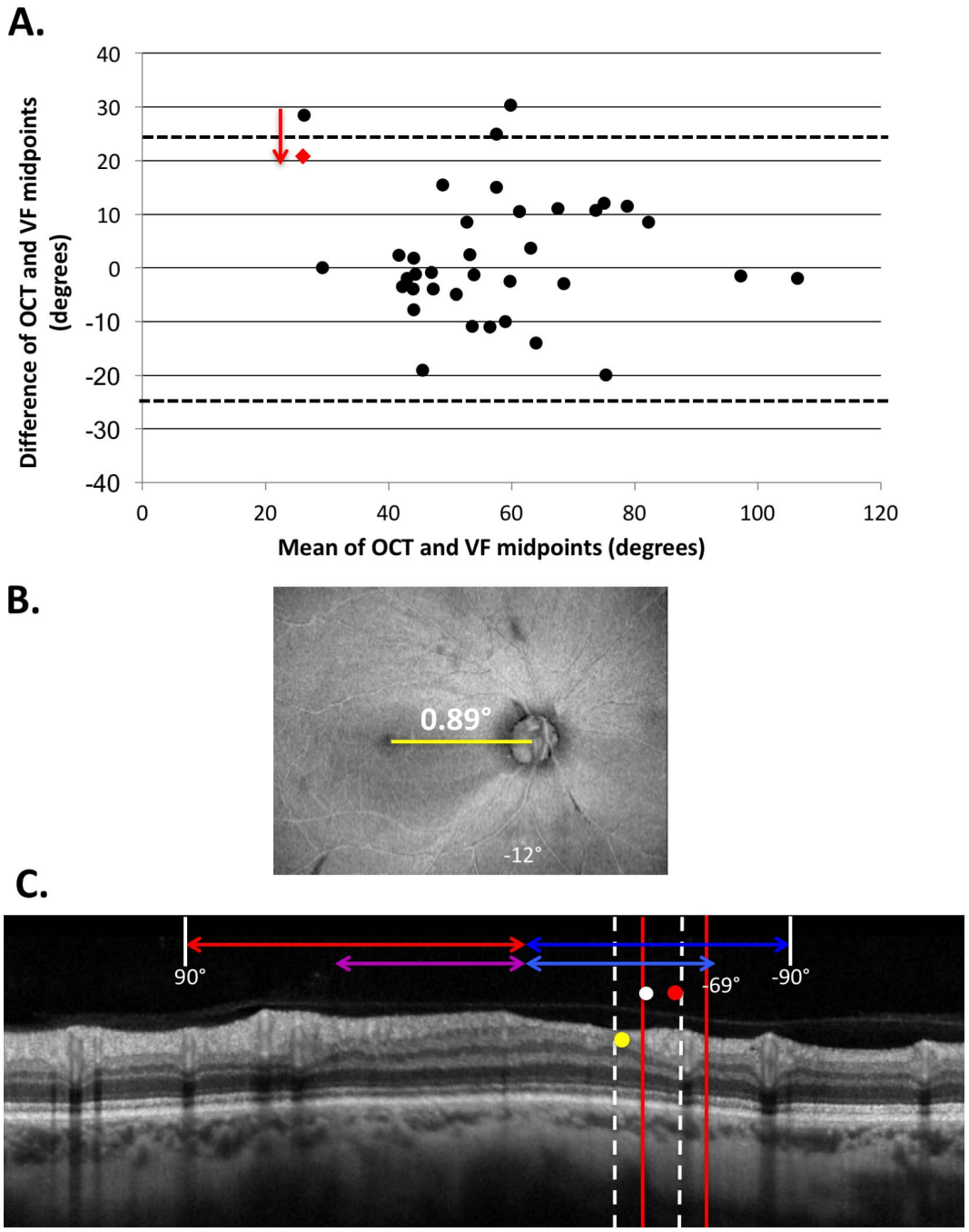

Figure 4. (**A**) Bland-Altman plot reflecting the agreement between the midpoint of the VF-predicted defect and the midpoint of the region of thinnest cpRNFL. The agreement was near identical for both pre- and post-adjustment for disc-to-fovea angle (95% limits of agreement ±23.6° and ±23.7°, respectively, shown by the *dotted horizontal lines*). The *black circles* represent preadjusted data and the *red dot* represents the post-adjusted result of the eye whose agreement improved by the correction. (**B**) En face projection of an eye that exhibited the smallest disc-to-fovea angle in the cohort. (**C**) The OCT circle scan of the eye in (**B**) with both the VF-predicted region and midpoint of damage pre- (*red vertical lines and circle*) and post- (*white dotted vertical lines and white circle*) disc-to-fovea adjustment.

1% normative limits. We also observed that a deep VF defect was always present in eyes with complete or nearly complete local cpRNFL loss in our sample. In other words, deep cpRNFL defects were associated with deep VF losses in both location and extent. While we explicitly designed our study to avoid the point-by-point comparison paradigm of previous structure–function studies,[8,11,14,15] the paper by Ganeshrao et al.[15] is most relevant. Interestingly, they improved the structure–function correlation from 0.56 to 0.72 by selecting the 30° region of the disc with the largest cpRNFL defect. This finding supports the notion that structure and function correspond well if the focus is on local cpRNFL defects. Ganeshrao and colleagues[15] did so by selecting a 30° sector in the region of greatest damage. Similarly, we chose to compare only the region of deepest structural damage with that of deepest functional damage.

In our study, there were two eyes, however, that had a relatively thicker, although still abnormal, cpRNFL thickness

Investigative Ophthalmology & Visual Science

(>21 μm) in the region of VF-predicted damage. According to the anatomic model, the RGC axons entering the temporal half of the disc come from the retinal region within ±15° of the center of the fovea (dashed black circle, Fig. 1C), plus the region of the retina labeled as "temporal retina (nasal visual field)" in Figure 1C.[25] Because these two eyes only had one to two deep test point locations, and only on the 24-2 VF, it is reasonable to assume that the RGCs in other regions of the temporal retina are intact and sending healthy axons to the disc, thereby yielding a thicker cpRNFL profile.

Overall, we observed that adjustments for the disc-to-fovea angle of each eye had a negligible impact on the level of spatial agreement between deep structural and functional abnormalities at the population level. This was evaluated because the anatomic model assumes an average disc-to-fovea angle, meaning that any deviation from this angle for an individual eye may result in deviations in the prediction of the location of damage on the cpRNFL scan. However, the location of the thinnest cpRNFL fell outside the VF prediction in only two of 32 eyes; adjusting for disc-to-fovea angle improved the spatial agreement in only one of these eyes.

Limitations of this study include its qualitative nature, in which the location of thinnest cpRNFL damage was determined by grading OCT circle scans images alone. However, because we limited our evaluation to eyes with deep VF defects, most eyes had cpRNFL loss that was either complete or near complete, making the identification of the thinnest cpRNFL region relatively simple. This was evident in the level of intergrader agreement in the location of the thinnest cpRNFL, with the limits of agreement falling within half a clock-hour sector. Another limitation of this study is its relatively small sample size, although these findings provide an initial estimate of the level of spatial agreement between structure and function in a careful manner, and the graders were masked to the results of each modality.

Despite these caveats, our findings provide important insights into the interpretation of the results of VF and OCT testing in eyes with deep visual field defects, and could be extrapolated with care when evaluating eyes with a less severe extent of glaucomatous damage. In this study, we used a population-based anatomic model to demonstrate that deep structural and functional loss exhibited 95% limits of agreement within two-thirds of a clock hour spatially. This finding could be used when evaluating eyes where diagnostic uncertainty exists. For example, cases in which mild repeatable VF defects are accompanied by structural loss within two-thirds of a clock hour as predicted by the anatomic model should provide greater confidence in glaucoma diagnosis. However, future studies are required to evaluate the validity of such an approach.

In conclusion, this study demonstrates that the 95% limits of spatial agreement between deep structural and functional glaucomatous defects fell within two-thirds of a 30° clock hour. These findings provide important insights into the interpretation of VF and OCT results in a clinically relevant context in the management of patients with glaucoma, and could potentially be used to improve diagnostic certainty in the earlier stages of this disease.

Acknowledgments

Supported by National Eye Institute (NEI) RO1-EY-02115 (Bethesda, MD, USA), NEI EY025253, The Crowley Family Fund of the New York Eye and Ear Infirmary of Mount Sinai (New York, NY, USA); a National Health and Medical Research Council Early Career Fellowship (#1104985, ZW; Canberra, Australia).

Disclosure: **M.A. Mavrommatis**, None; **Z. Wu**, None; **S.I. Naegele**, None; **J. Nunez**, None; **C.G. De Moraes**, None; **R. Ritch**, None; **D.C. Hood**, Topcon, Inc. (C, F, R); Heidelberg Engineering, Inc. (C, F, R); Novartis (C, F, R)

References

1. Weinreb RN, Khaw PT. Primary open-angle glaucoma. *Lancet*. 2004;363:1711–1720.
2. Prum BE, Rosenberg LF, Gedde SJ, et al. Primary open-angle glaucoma preferred pattern guidelines. *Ophthalmology*. 2015;123:41–111.
3. Sharma P, Sample PA, Zangwill LM, Schuman JS. Diagnostic tools for glaucoma detection and management. *Ophthalmology*. 2008;53:S17–S32.
4. Wollstein G, Schuman JS, Price LL. Optical coherence tomography longitudinal evaluation of retinal nerve fiber layer thickness in glaucoma. *Arch Ophthalmol*. 2005;123:464–470.
5. Costa RA, Skaf M, Melo LAS Jr, et al. Retinal assessment using optical coherence tomography. *Prog Retin Eye Res*. 2006;25:325–353.
6. van Velthoven MEJ, Faber DJ, Verbraak FD, van Leeuwen TG, de Smet MD. Recent developments in optical coherence tomography for imaging the retina. *Prog Retin Eye Res*. 2007;26:57–77.
7. Hood DC, Kardon RH. A framework for comparing structural and functional measures of glaucomatous damage. *Prog Retin Eye Res*. 2007;26:688–710.
8. Malik R, Swanson WH, Garway-Heath DF. The 'structure-function' relationship in glaucoma - past thinking and current concepts. *Clin Exp Ophthalmol*. 2012;40:369–380.
9. Garway-Heath DF, Poinoosawmy D, Fitzke FW, Hitchings RA. Mapping the visual field to the optic disc in normal tension glaucoma eyes. *Ophthalmology*. 2000;107:1809–1815.
10. Medieros FA, Zangwill LM, Bowd C, Mansouri K, Weinreb RN. The structure and function relationship in glaucoma; implications for detection of progression and measurement of rates of change. *Invest Ophthalmol Vis Sci*. 2012;53:6939–6946.
11. Anderson RS. The psychophysics of glaucoma: improving the structure-function relationship. *Prog Retin Eye Res*. 2006;25:79–97.
12. Hood DC, Anderson SC, Wall M, Raza AS, Kardon RH. A test of a linear model of glaucomatous structure-function loss reveals sources of variability in retinal nerve fiber and visual field measurements. *Invest Ophthalmol Vis Sci*. 2009;50:4254–4266.
13. Hood DC, Anderson SC, Wall M, Kardon RH. Structure versus function in glaucoma: an application of a linear model. *Invest Ophthalmol Vis Sci*. 2007;48:3662–3668.
14. Denniss J, Turpin A, McKendrick AM. Individualized structure-function mapping for glaucoma: practical constraints on map resolution for clinical and research applications. *Invest Ophthalmol Vis Sci*. 2014;55:1985–1993.
15. Ganeshrao SB, Turpin A, Denniss J, McKendrick AM. Enhancing structure-function correlations in glaucoma with customized spatial mapping. *Ophthalmology*. 2015;122:1695–1705.
16. Horn FK, Mardin CY, Laemmer R, et al. Correlation between local glaucomatous visual field defects and loss of nerve fiber layer thickness measured with polarimetry and spectral domain OCT. *Invest Ophthalmol Vis Sci*. 2009;50:1971–1977.
17. Rao H, Zangwill LM, Weinreb RN, et al. Structure-function relationship in glaucoma using spectral-domain optical coherence tomography. *Arch Ophthalmol*. 2011;129:864–871.
18. Leite MT, Zangwill LM, Weinreb RN, et al. Structure-function relationships using the Cirrus spectral domain optical

coherence tomograph and standard automated perimetry. *J Glaucoma*. 2012;21:49–54.

19. Pinto LM, Costa EF, Melo LAS Jr, et al. Structure-function correlations in glaucoma using matrix and standard automated perimetry versus time-domain and spectal-domain OCT devices. *Invest Ophthalmol Vis Sci*. 2014;55:3074–3080.
20. Hood DC, Raza AS. Method for comparing visual field defects to local RNFL and RGC damage seen on frequency domain OCT in patients with glaucoma. *Biomed Opt Express*. 2011;2: 1097–1105.
21. Hood DC, Raza AS, de Moraes CGV, et al. Initial arcuate defects within the central 10 degrees in glaucoma. *Invest Ophthalmol Vis Sci*. 2011;52:940–946.
22. Raza AS, Cho J, de Moraes CGV, et al. Retinal ganglion cell layer thickness and local visual field sensitivity in glaucoma. *Ophthalmology*. 2011;129:1529–1536.
23. Drasdo N, Millican CL, Katholi CR, Curcio CA. The length of Henle fibers in the human retina and a model of ganglion receptive field density inthe visual field. *Vision Res*. 2007;47: 2901–2911.
24. Hood DC, Raza AS, de Moraes CGV, Liebmann JM, Ritch R. Glaucomatous damage of the macula. *Prog Retin Eye Res*. 2013;32:1–21.
25. Hood DC. Improving our understanding, and detection, of glaucomatous damage: an approach based upon optical coherence tomography (OCT). *Prog Retin Eye Res*. 2016;57: 46–57.
26. Jansonius NM, Schiefer J, Nevalainen J, Paetzold J, Schiefer U. A mathematical model for describing the retinal nerve fiber bundle trajectories in the human eye: average course, variability, and influence of refraction, optic disc size and optic disc position. *Exp Eye Res*. 2012;105:70–78.

Investigative Ophthalmology & Visual Science